Mol Neurobiol (2012) 45:550–563
DOI 10.1007/s12035-012-8274-9

Deregulation of BRCA1 Leads to Impaired Spatiotemporal Dynamics of γ-H2AX and DNA Damage Responses in Huntington's Disease

Gye Sun Jeon · Ki Yoon Kim · Yu Jin Hwang · Min-Kyung Jung · Sungkwan An · Mutsuko Ouchi · Toru Ouchi · Neil Kowall · Junghee Lee · Hoon Ryu

Received: 28 February 2012 / Accepted: 26 April 2012 / Published online: 13 May 2012

Abstract Huntington's disease (HD) is an autosomal dominant neurodegenerative disorder of mid-life onset characterized by involuntary movements and progressive cognitive decline caused by a CAG repeat expansion in exon 1 of the *Huntingtin* (*Htt*) gene. Neuronal DNA damage is one of the major features of neurodegeneration in HD, but it is not known how it arises or relates to the triplet repeat expansion mutation in the *Htt* gene. Herein, we found that imbalanced levels of non-phosphorylated and phosphorylated BRCA1 contribute to the DNA damage response in HD. Notably, nuclear foci of γ-H2AX, the molecular component that recruits various DNA damage repair factors to damage sites including BRCA1, were deregulated when DNA was damaged in HD cell lines. BRCA1 specifically interacted with γ-H2AX via the BRCT domain, and this association was reduced in HD. BRCA1 overexpression restored γ-H2AX level in the nucleus of HD cells, while BRCA1 knockdown reduced the spatiotemporal propagation of γ-H2AX foci to the nucleoplasm. The deregulation of BRCA1 correlated with an abnormal nuclear distribution of γ-H2AX in striatal neurons of HD transgenic (R6/2) mice and BRCA1$^{+/-}$ mice. Our data indicate that BRCA1 is required for the efficient focal recruitment of γ-H2AX to the sites of neuronal DNA damage. Taken together, our results show that BRCA1 directly modulates the spatiotemporal dynamics of γ-H2AX upon genotoxic stress and serves as a molecular maker for neuronal DNA damage response in HD.

Keywords DNA damage · BRCA1 · H2AX · Neurodegeneration · Huntington's disease

Electronic supplementary material The online version of this article (doi:10.1007/s12035-012-8274-9) contains supplementary material, which is available to authorized users.

G. S. Jeon · K. Y. Kim · Y. J. Hwang · M.-K. Jung · H. Ryu
WCU Neurocytomics Group, Department of Biomedical Sciences, Seoul National University College of Medicine, Seoul 110-799, South Korea

S. An
Department of Microbial Engineering, Functional Genoproteome Research Center, Konkuk University, Seoul, South Korea

M. Ouchi · T. Ouchi
Pritzker School of Medicine, Systems Biology Program, NUHS, University of Chicago, Evanston, IL, USA

M. Ouchi · T. Ouchi
Department of Cancer Genetics, Roswell Park Cancer Institute, Buffalo, NY 14263, USA

N. Kowall · J. Lee · H. Ryu
VA Boston Healthcare System, Boston, MA 02130, USA

N. Kowall · J. Lee · H. Ryu
Boston University Alzheimer's Disease Center, Boston University School of Medicine, Boston, MA 02118, USA

N. Kowall · J. Lee · H. Ryu (✉)
Department of Neurology, Boston University School of Medicine, 150 South Huntington Ave., Boston, MA 02118, USA
e-mail: hoonryu@bu.edu

Introduction

Huntington's disease (HD) is an autosomal dominant disorder characterized by chorea and progressive cognitive impairment caused by a CAG repeat expansion in exon 1 of the *Huntingtin* (*Htt*) gene. Cumulative neuronal DNA damage due to impaired DNA repair mechanisms is thought to contribute to the pathogenesis of HD and other neurodegenerative disorders [1, 2], but the potential role of the DNA damage response (DDR) in the pathogenesis of HD is not understood.

The breast cancer susceptibility gene *BRCA1* encodes a large phosphoprotein involved in multiple nuclear functions, including DNA repair, transcriptional regulation, and chromatin remodeling ([3]; for review see [4–7]). BRCA1 is phosphorylated in a cell cycle-dependent manner, and several phosphorylation sites have been identified under these conditions, including Ser-988, -1423, -1387, and -1524 [8, 9]. In response to DNA damage, the BRCA1 protein becomes rapidly hyperphosphorylated at multiple sites by several kinases including ATM, a gene mutated in the ataxia telangiectasia syndrome. Mutation of the BRCA1 target sites for ATM and serines 1423 and 1524 abolishes the ability of BRCA1 to mediate the G2/M checkpoint, while mutation at serine 1387 disrupts the S-phase checkpoint. Interestingly, overexpression of wild-type BRCA1 confers weak resistance to DNA damage-induced cell death in BRCA1 mutant breast cancer cell lines, whereas phosphorylation-defective BRCA1 alleles carrying Ser to Ala substitution of these residues do not rescue them from apoptosis [10–12]. Thus, DNA damage-induced phosphorylation of BRCA1 is an intracellular signal that orchestrates cell survival and death pathways. Mutations of mouse BRCA1 using various gene-targeting constructs that introduce null, hypomorphic, and tissue-specific mutations result in embryonic lethality, cellular growth defects, increased apoptosis, premature aging, and/or tumorigenesis [13–24].

The DDR is essential for the development, maintenance, and normal functioning of the adult central nervous system. H2AX is a member of the mammalian histone H2A family (for review see [25]). H2AX is phosphorylated (γ-H2AX) and relocated to double-strand breaks (DSBs) within minutes of genotoxic stress, which suggests that γ-H2AX may play a crucial role in DSB repair [26]. Indeed, γ-H2AX is the molecular component that recruits various DNA damage repair factors to damage sites including BRCA1 [26–29]. Despite the fact that interactions between BRCA1 and γ-H2AX are important in the DNA repair process, the mechanism of interaction of these two molecules has not been thoroughly investigated in neurodegenerative conditions such as HD.

The aim of our study was to address how BRCA1 and H2AX interact and contribute to the DDR in HD. We found that an imbalance between levels of non-phosphorylated and phosphorylated BRCA1 leads to dysregulation of the spatiotemporal dynamics of γ-H2AX, which, in turn, results in failure of the DNA damage response in HD.

Results

The Level of Non-phosphorylated and Phosphorylated ATM and BRCA1 Is Altered in a Cellular and Animal Model of HD

In the first series of experiments, we determined whether levels of ATM and BRCA1 differ between control ST*Hdh*$^{Q7/7}$ (Q7) and mutant HD ST*Hdh*$^{Q111/111}$ (Q111) cells by Western blot and immunohistochemistry. Levels of non-phosphorylated ATM and phosphorylated ATM (p-ATM (Ser1981)) were slightly but not significantly increased in Q111 cells compared to Q7 cells (Fig. 1a). ATM and p-ATM (Ser1981) signals were found both in the cytoplasm and the nucleus of striatal cell lines. A substantial portion of the ATM signal appeared to be localized to the nuclei of striatal cells, whereas p-ATM (Ser1981) was present in the nuclei as well as in the cytoplasm (Fig. 1b). The R6/2 line is a transgenic HD mouse line expressing exon 1 of the mutant human HD gene with an expanded CAG repeat [30] that develops neuropathological and clinical features similar to human HD including striatal atrophy and neuronal intranuclear inclusions. Levels of ATM and p-ATM (Ser1981) were slightly increased in the striatum of R6/2 mice at 10 weeks of age compared to littermate controls, as monitored by immunohistochemistry (Fig. 1c). Interestingly, levels of non-phosphorylated BRCA1 were significantly decreased in Q111 cells compared to Q7 cells, whereas phosphorylated BRCA1 (p-BRCA1 Ser 1423 and Ser 1524) was significantly increased in Q111 cells compared to Q7 cells (Fig. 1d). BRCA1 and p-BRCA1 (Ser1423) were localized to the cytoplasm of striatal cells, whereas p-BRCA1 (Ser1524) was mainly localized in the nucleus (Fig. 1e). The immunoreactivity of p-BRCA1 (Ser 1423 and Ser 1524) was increased, while non-phosphorylated BRCA1 immunoreactivity was decreased in the striatum of R6/2 mice compared to littermate controls (Fig. 1f). To determine whether BRCA1 was affected in vivo, we examined ATM, BRCA1, p-BRCA1 (Ser1524), and γ-H2AX protein levels in striatal neurons stably expressing GFP or the mutant huntingtin-GFP fusion protein (GFP-Q79) and found that these protein levels were similar to those found in a cellular and animal model of HD [Fig. 1 in the Electronic Supplementary Material (ESM)].

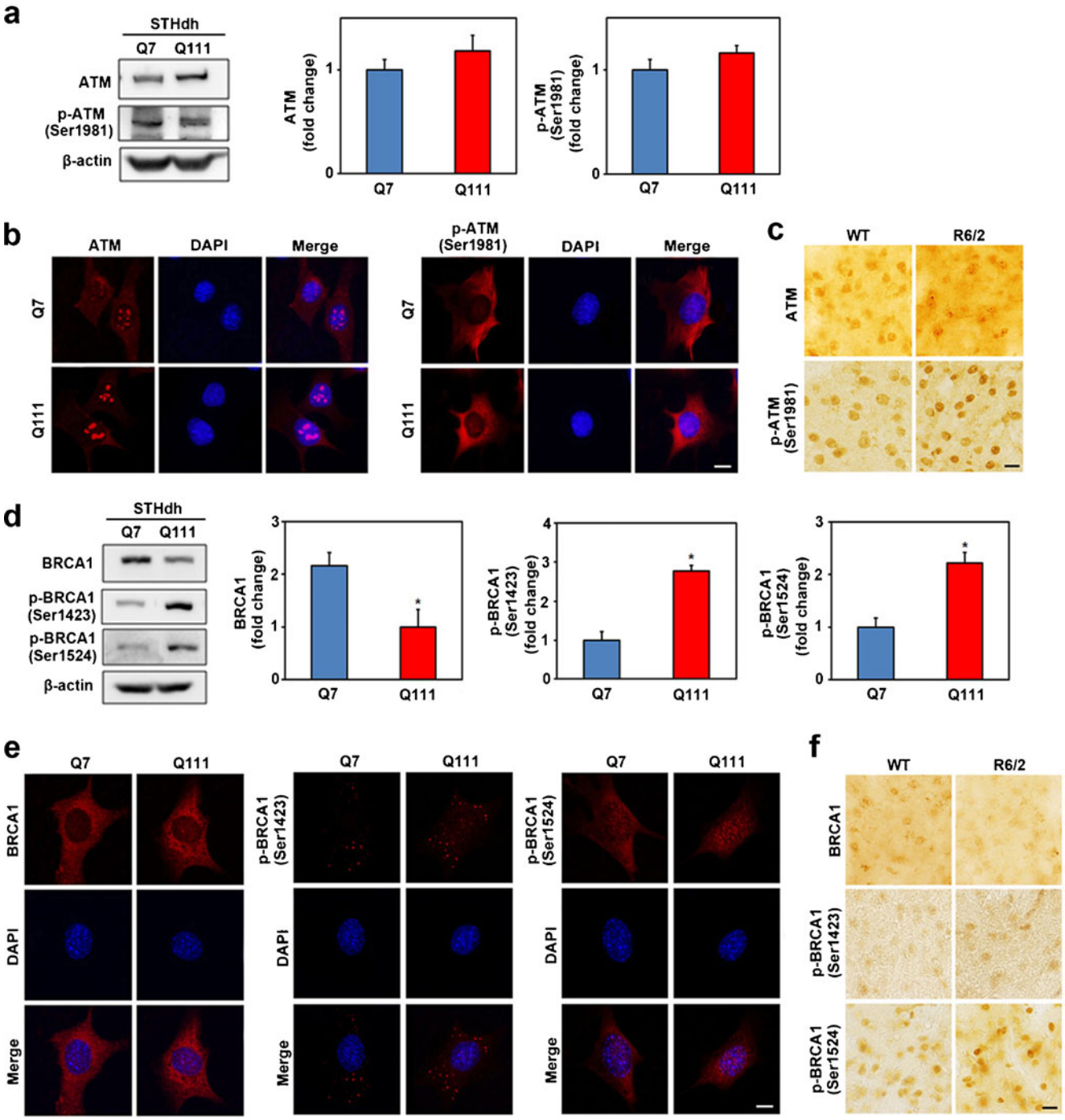

Fig. 1 Non-phosphorylated and phosphorylated forms of ATM and BRCA1 are altered in a cellular and an animal model of HD. **a** The protein level of ATM, p-ATM (Ser1981), and β-actin in ST*Hdh*$^{Q7/7}$ (Q7) and ST*Hdh*$^{Q111/111}$ (Q111) cells was detected by Western blot analysis. The graphed data represent an average of four separate experiments. **b** ATM and p-ATM (Ser1981) immunoreactivity was found both in the cytoplasm and nuclei of striatal cell lines. **c** Levels of ATM and p-ATM (Ser1981) were slightly increased in the striatum of R6/2 mice at 10 weeks of age compared to littermate controls. **d** Protein levels of BRCA1, p-BRCA1 (Ser1423), p-BRCA1 (Ser1524), and β-actin in Q7 and Q111 cells were detected by Western blot analysis. The data represent an average of four separate experiments. *$p<0.05$, significantly different from control. **e** BRCA1 and p-BRCA1 (Ser1423) immunoreactivity was seen in the cytoplasm, in contrast to p-BRCA1 (Ser1524) which was localized in the nuclei of striatal cells. **f** Phosphorylated forms of BRCA1 were increased in the striatum of R6/2 mice compared to littermate controls, while levels of non-phosphorylated BRCA1 were lower in the striatum of R6/2 mice. *Scale bars*: **b**, **c**, **e**, **f**, 10 μm

CPT-Induced DNA Damage Alters the Expression of ATM, BRCA1, and H2AX Pathway in the Cellular Model of HD

In order to examine whether altered BRCA1 levels affect the DNA damage pathway, we exposed striatal cell lines to camptothecin (CPT), a topoisomerase inhibitor, up to 10 μM for 24 h and investigated changes in the DNA damage responses. Upon CPT-induced DNA damage, we determined ATM activation by assessing ATM (ser1981) phosphorylation with Western blot analysis (Fig. 2a). ATM phosphorylation was significantly increased 3 h after the induction of DNA damage, and BRCA1 phosphorylation at Ser 1423 and 1524 was increased 3–6 h after the DNA damage (Fig. 2b). These data show that activation of ATM and the BRCA1 pathway is impaired in a HD cell line in response to DNA damage. We next evaluated whether a downstream target of ATM, such as H2AX, is deregulated in the context of DNA damage. Phosphorylated H2AX on Ser140 (γ-H2AX) is a sensitive indicator of DNA double-strand breaks produced by genotoxic stresses. Western blot experiments showed that CPT-induced DNA damage response as measured by γ-H2AX levels is evident at 3 h and increased up to 6 h (Fig. 2c). To further determine how CPT-induced DNA damage is associated with cell death in a cellular model of HD, Q7 and Q111 cells were treated with CPT and analyzed by flow cytometry (FACS). As shown in Fig. 2d, CPT (10 μM) treatment causes apoptotic cell death both in Q7 and Q111 cells. As expected, there was an increase in apoptotic cell death from 12 to 41 % in Q7 control cells and from 18 to 52 % in Q111 HD cells, respectively. In addition, neuronal DNA damage caused by genotoxic stress was examined in terms of DNA double-stand breaks by terminal deoxynucleotidyl transferase dUTP nick end labeling (TUNEL) staining along with 4′,6-diamidino-2-phenylindole (DAPI) counterstaining. Our results show that Q111 HD cells are more sensitive to DNA damage caused by CPT compared to Q7 control cells (Fig. 2e). The typical apoptotic morphology of nuclei was seen in both Q7 and Q111 cells after 12 or 24 h of CPT treatment. As expected, however, DNA double-strand breaks were significantly increased in Q111 cells compared to Q7 cells in a time-dependent manner.

Differential Subcellular Localization of ATM, BRCA1, and H2AX Is Found in the Cellular Model of HD

Because subcellular localization is an important factor related to protein function, we investigated the distribution of ATM, BRCA1, and γ-H2AX in striatal cells. Interestingly, ATM and BRCA1 were found in both the nucleus and cytosol of striatal cell lines (Q7 and Q111 cells). High levels of γ-H2AX protein were found in nucleoli, and its basal level was higher in Q7 cells than Q111 cells (Fig. 3a). γ-H2AX immunoreactivity was in the form of punctate structures in cellular nuclei. When cells were exposed to DNA damage for 3 h, the γ-H2AX foci were diffusely redistributed in the nuclei of Q7 and Q111 cells (Fig. 3b). However, the immunoreactivity of the nuclear γ-H2AX foci was lowered in Q111 HD cells compared to Q7 cells in response to DNA damage. Knockdown of BRCA1 by expressing EGFP-shRNA BRCA1 constructs inhibited the spatial redistribution of γ-H2AX in the nucleus after CPT treatment in normal cells (Fig. 3c). It is noteworthy that γ-H2AX was mainly increased in both the nucleus and nucleoli 3 h after CPT treatment (Fig. 3c). BRCA1 knockdown resulted in a marked attenuation of the γ-H2AX signal induced by CPT in Q111 cells compared to Q7 cells (Fig. 3d). While the nuclear γ-H2AX signal increased and persisted for more than 6 h after CPT-induced DNA damage, its signal did not last more than 3 h in Q111 HD cells. Thus, the depletion of endogenous BRCA1 was coupled to a reduction of γ-H2AX-positive foci upon CPT treatment in Q111 HD cells. This finding strongly supports a role for BRCA1 in the maintenance of DDR via γ-H2AX. We further found that p-BRCA1 (Ser1524) and γ-H2AX are differently localized in Q7 and Q111 cells (Fig. 3e). Confocal microscopy revealed that p-BRCA1 (Ser1524) and γ-H2AX immunoreactivity are both increased in the nucleoplasm after CPT-induced DNA damage. A histogram analysis of the γ-H2AX signal in the nucleus of CPT-treated cells revealed that p-BRCA1 (Ser1524) foci are strongly associated with the γ-H2AX signal in Q7 cells, whereas p-BRCA1 (Ser1524) foci are only partially associated with γ-H2AX in Q111 cells (Fig. 3e).

Genotoxic Stress-Induced Interaction of BRCA1 and γ-H2AX Is Impaired in the Cellular Model of HD

To further characterize the molecular interactions of ATM, BRCA1, and H2AX, we performed immunoprecipitations on neuronal lysates, using anti-ATM, anti-BRCA1, or anti-H2AX antibodies (Fig. 4a). A prominent 17-kDa band of H2AX protein was present in both ATM and BRCA1 immunoprecipitations. The molecular interaction of H2AX with ATM or BRCA1 was apparent in both Q7 and Q111 cells. We also confirmed that ATM, BRCA1, and H2AX interact constitutively to generate a DDR complex in neurons (Fig. 4a). In order to examine whether DNA damage modulates the association of γ-H2AX with p-BRCA1 (Ser1524), we prepared cell lysates from mCherry-H2AX transfected Q7 and Q111 cells after CPT treatment and performed co-immunoprecipitations. The constitutive association of γ-H2AX with p-BRCA1 (Ser1524) was found in Q7 cells but not in Q111 cells under normal condition without CPT treatment. An increase in the association of γ-H2AX with p-BRCA1 (Ser1524) was found in Q111 cells

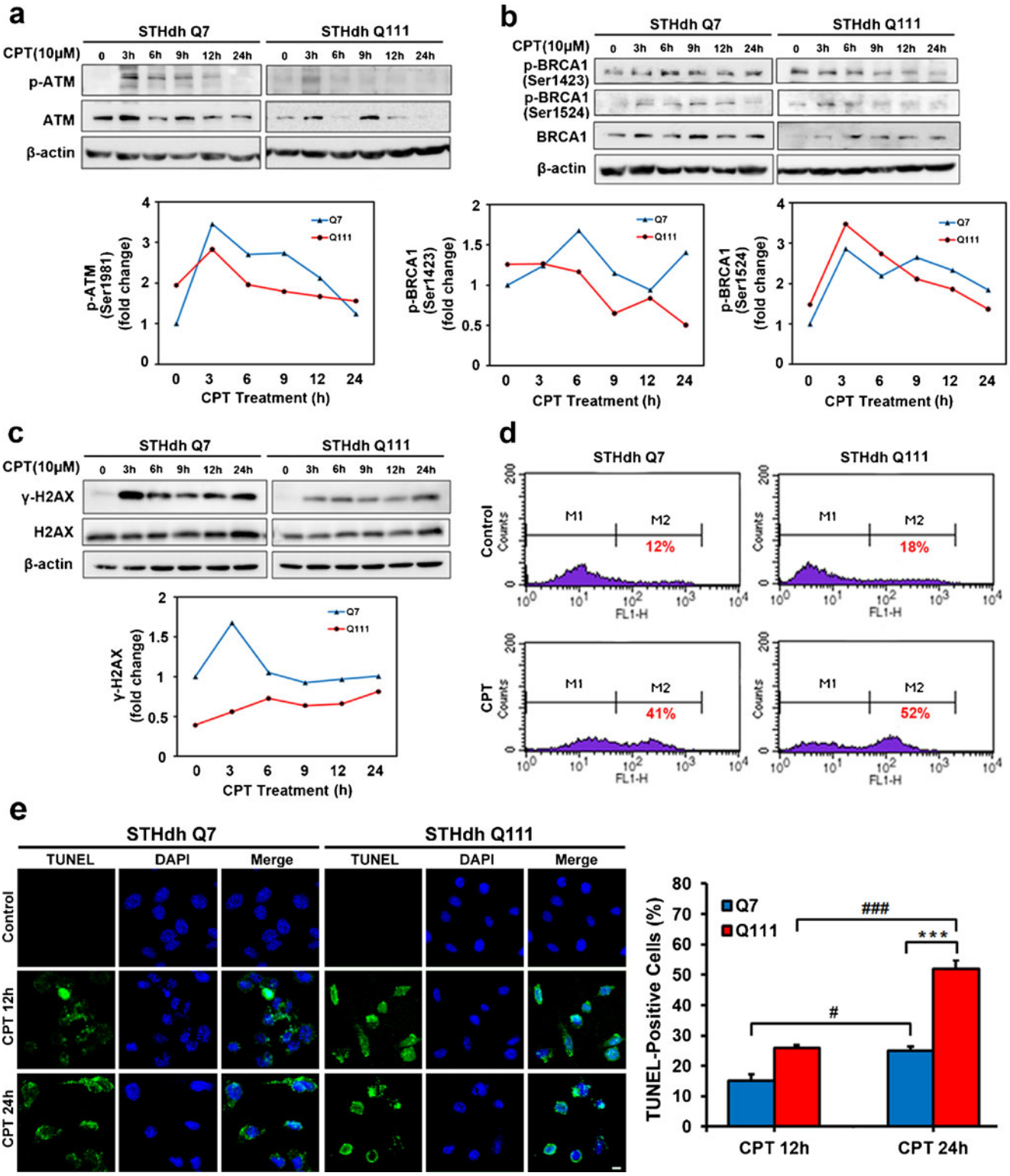

Fig. 2 Activation of ATM, BRCA1, and H2AX pathway by genotoxic stress (camptothecin-induced DNA damage) is deregulated in the cellular model of HD. **a** The phosphorylation of ATM by camptothecin (CPT) was reduced in Q111 cells compared to Q7 cells. Cells were treated with CPT (10 μM) for the indicated period of time. **b** The phosphorylation of BRCA1 at Ser1423 and S1524 by CPT was differentially regulated in between Q7 and Q111 cells. **c** The phosphorylation of H2AX at Ser140 was deregulated in Q111 cells. The data represent an average of three separate experiments (**a**–**c**). **d** CPT-induced DNA damage led to apoptotic cell death in Q7 and Q111 cells as measured by flow cytometry. **e** DNA double-strand breaks were increased in Q111 HD cells. In situ apoptotic TUNEL detection is represented by *green* labeling in contrast to DAPI (*blue*) counterstaining of all nuclei. *Scale bars*: 10 μm. The TUNEL-positive cells were examined under an epifluorescence microscope at ×20 objective magnification. The data represent an average of counting from four separate areas. Significantly different at $^{\#}p<0.05$; $^{\#\#\#}p<0.001$; $^{***}p<0.001$

3 h after CPT treatment. A stronger association of p-BRCA1 (Ser1524) with γ-H2AX was found in Q7 cells than in Q111 cells after CPT treatment (Fig. 4b). To determine whether γ-H2AX directly binds to BRCA1 and to identify which site of BRCA1 interacts with γ-H2AX, a GST pull-down assay was performed on cell lysates with or without CPT treatment. We purified six glutathione *S*-transferase (GST)-BRCA1 fusion proteins (numbered 1–6) containing overlapping BRCA1 fragments. Among the six GST-BRCA1 fusion proteins, γ-H2AX most strongly interacted with the BRCT domains of BRCA1 (BRCA1 amino acids 1314–1863; Fig. 4c). Moreover, CPT treatment increased the ability of γ-H2AX binding to BRCT domains of BRCA1 in a concentration-dependent manner in Q7 and Q111 cells (Fig. 4d). CPT treatment enhanced the association of γ-H2AX with the BRCT domain in Q7 cells more than in Q111 cells. These data indicate that the association of γ-H2AX with BRCA1 is lacking in HD Q111 cells. We performed further GST-BRCA1 pull downs using cell lysates containing WT-H2AX, mutant H2AX (S140A), and mutant H2AX (S140E), respectively. Mutation of H2AX at Ser140 hindered its association with BRCA1, indicating that phosphorylation of Ser140 is important for its molecular interaction with BRCA1 (Fig. 4e).

Spatial Distribution of γ-H2AX in the Nucleus Is Dysregulated in HD

To determine whether the amount and spatial distribution of γ-H2AX in the nucleus are affected in vivo, we examined the immunoreactivity of γ-H2AX in the striatum of the R6/2 transgenic mouse model. Levels of γ-H2AX were markedly decreased in the cortex and striatum of R6/2 mice (10 weeks old) compared to littermate controls (Fig. 5a). γ-H2AX was mainly present in nucleoli that were positively stained with UBF, a well-known nucleolus marker. Punctate γ-H2AX immunoreactivity was mainly colocalized with UBF in nucleolar regions (Fig. 5c). p-BRCA1 (Ser1524) immunoreactivity was markedly increased in striatal neurons of R6/2 mice compared to wild-type littermate control mice at 10 weeks of age. p-BRCA1 (Ser1524) and mtHtt were not co-localized (Fig. 2 in the ESM). Interestingly, γ-H2AX immunoreactivity was decreased in the cortex and striatum of BRCA1 heterozygous knockout ($BRCA1^{+/-}$) mice compared to WT ($BRCA1^{+/+}$) mice, similar to the pattern we found in R6/2 HD mice (Fig. 5b). Confocal microscopy revealed that p-BRCA1 (Ser1524) and γ-H2AX are colocalized in striatal neurons of WT mice. Quantitative analysis of fluorescence intensity confirmed that the γ-H2AX signal was spatially colocalized with the p-BRCA1 (Ser1524) signal in the nuclei of striatal neurons of littermate control mice, whereas γ-H2AX was not colocalized with p-BRCA1 (Ser1524) in striatal neurons of R6/2 HD mice (Fig. 5d).

Fig. 3 Differential subcellular localizations of ATM, BRCA1, and H2AX are found in the cellular model of HD. **a** γ-H2AX levels were reduced in the nucleoli of Q111 cells compared to Q7 cells. **b** CPT-induced DNA damage modulated spatiotemporal changes of γ-H2AX foci in the nucleus of Q7 and Q111 cells. Cells were treated with CPT (10 μM) for 3 h. **c** Knockdown of BRCA1 by shRNA altered the activation and the subcellular localization of γ-H2AX. **d** Knockdown of BRCA1 resulted in a marked attenuation of the γ-H2AX signal by CPT in Q111 cells compared to Q7 cells. **e** The level of p-BRCA1 (Ser1524) and γ-H2AX was differentially regulated in the nucleoplasm of Q7 and Q111 cells in response to CPT. *Upper panel*: images taken by confocal microscopy, *lower panel*: histogram analysis of the γ-H2AX images derived from the *upper panel*. *Scale bars*: **b** and **e**, 10 μm

BRCA1 Directly Regulates the Spatiotemporal Propagation of γ-H2AX to the Nucleoplasm

Since we found that BRCA1 directly interacts with γ-H2AX through the BRCT domain, we hypothesized that BRCA1 directly regulates the spatiotemporal dynamics of γ-H2AX in response to DNA damage. First, we overexpressed WT-BRCA1 in HD cells (Q111) and found that BRCA1 restores γ-H2AX levels in response to CPT-induced DNA damage response in both Q111 and Q7 cells. Phosphorylation site mutant BRCA1 (Ser 1423/1524A) did not restore γ-H2AX levels under the DNA damage response (Fig. 6a). Next, we knocked down BRCA1 using shRNA BRCA1 and assessed the propagation of the γ-H2AX signal to the nucleoplasm to determine whether BRCA1 modulates the spatiotemporal dynamics of γ-H2AX or not. Confocal microscopy confirmed that BRCA1 knockdown (GFP-positive) cells exhibit an abnormal γ-H2AX spatiotemporal dynamic compared to shRNA control cells in response to genotoxic stress induced by CPT (Fig. 6b). BRCA1 deficiency failed to generate diffuse discrete foci of γ-H2AX in response to DNA damage (Fig. 6b). Based on these data, we propose a scheme that summarizes our major findings, i.e., that the phosphorylation status of BRCA1 is imbalanced in normal versus HD striatal cells and that BRCA1-dependent spatiotemporal dynamics of γ-H2AX is impaired in HD cells (Fig. 7).

Discussion

The neuronal DDR is a key element contributing to the pathogenesis of polyQ diseases such as HD, but how it does so is not clear [31, 32]. Understanding the multiple pathogenic pathways and target molecules that underlie DNA repair may lead to the development of new therapeutic approaches to HD. In this study, we present two main findings: (1) the phosphorylation status of BRCA1 is imbalanced in HD striatal cells and (2) BRCA1-dependent

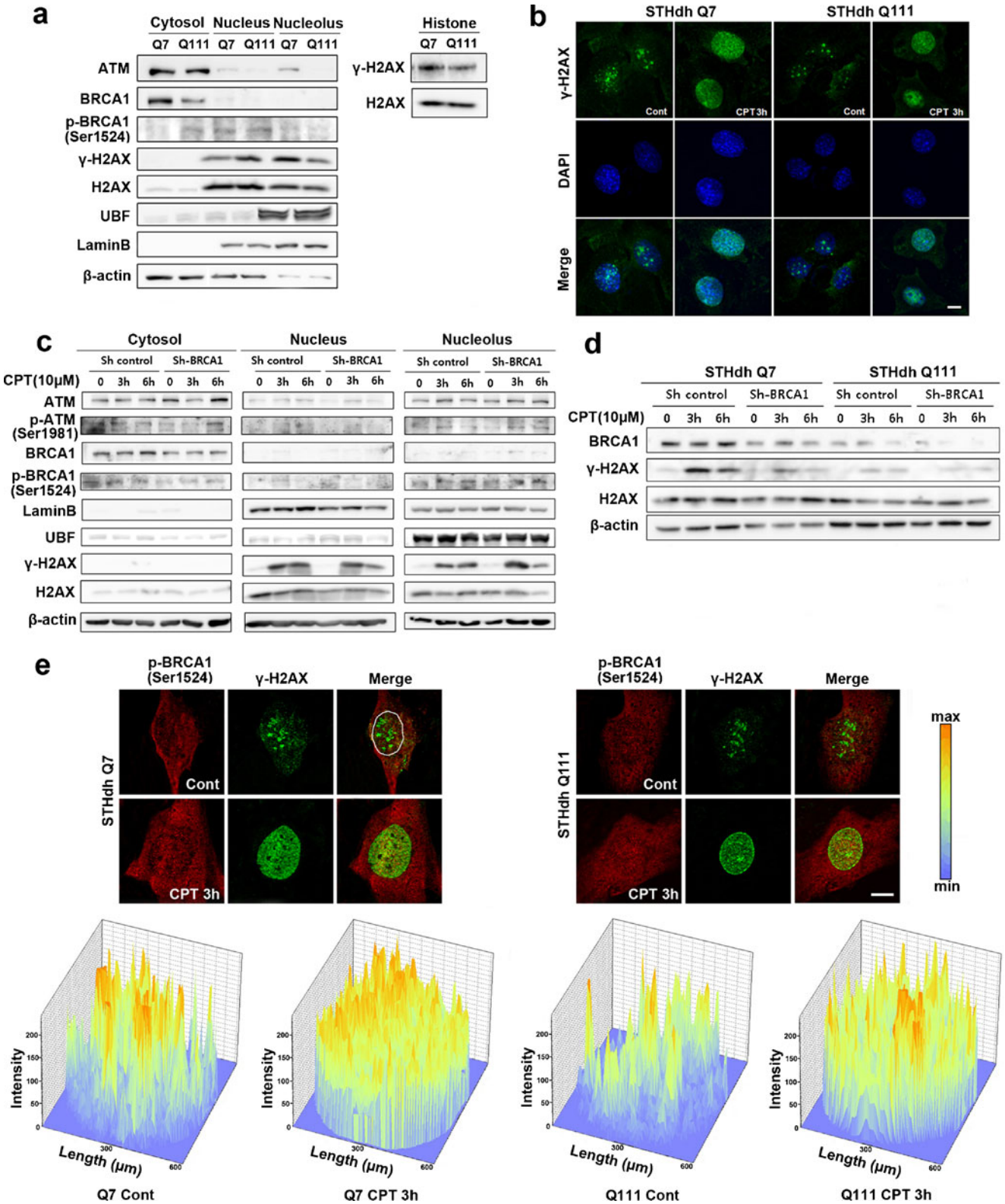

spatiotemporal dynamics of γ-H2AX is impaired in HD cells, and, as a result, BRCA1-γ-H2AX-associated DNA repair is dysfunctional, and DNA damage is enhanced in HD cells under genotoxic stress.

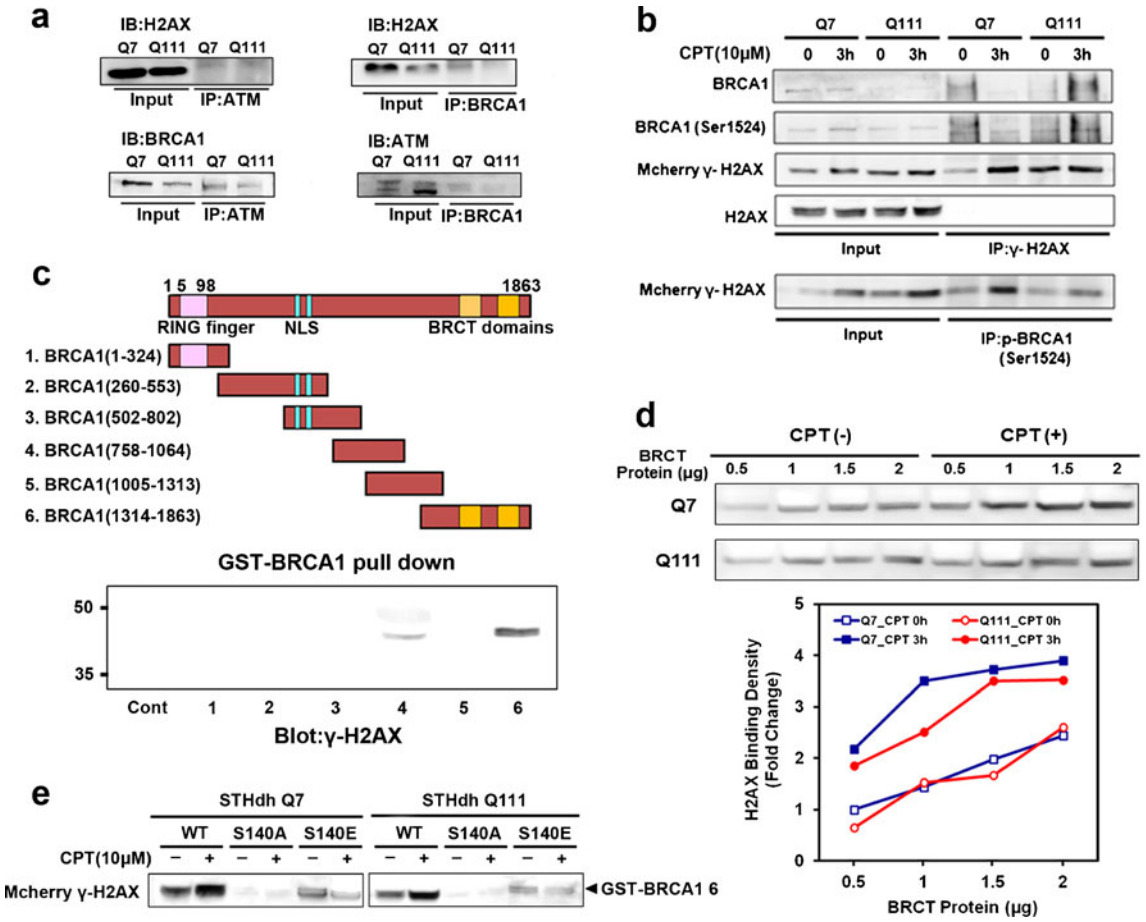

Fig. 4 Genotoxic stress-induced interaction of BRCA1 and γ-H2AX is impaired in the cellular model of HD. **a** The molecular interaction of H2AX with ATM and BRCA1 was apparent in both Q7 and Q111 cells. **b** The binding of γ-H2AX with p-BRCA1 (Ser1524) was increased by CPT-induced DNA damage. mCherry-H2AX was transiently transfected to Q7 and Q111 cells. Cell lysates were prepared 3 h after CPT treatment and applied for immunoprecipitation (*IP*). **c** γ-H2AX interacted with the BRCT domain of BRCA1. GST-BRCA1 pull-down assay was performed with Q7 cell lysates. **d** The binding activity of H2AX to the BRCT domain of BRCA1 was decreased in Q111 HD cells compared to Q7 cells under CPT-induced DNA damage. The data represent an average of three separate experiments. **e** The phosphorylation of H2AX at Ser140 was a key event to interact with the BRCT domain of BRCA1. The GST-BRCA1 pull-down assay was performed with cell lysates from mCherry-H2AX transfected cells

BRCA1 Phosphorylation Is Altered in HD

The spatial association of BRCA1 to sites of DNA damage implies that it plays a role in DNA repair. Early stages of the cellular response to DNA damage are accompanied by the phosphorylation of BRCA1 at Ser1423 and Ser1524 by ATM kinase [33, 34]. The phosphorylation of Ser1423 and Ser1524 is thought to play a key role in the DDR because mutated BRCA1 protein lacking these two phosphorylation sites fail to prevent DNA damage. It is unclear how BRCA1 orchestrates the complex cascade of DDR. Upon DNA damage, BRCA1 is dispersed from the discrete foci and relocalized to DNA damage-induced foci. BRCA1 colocalizes in these damage-induced foci with a number of proteins involved in the DDR such as ATM and H2AX [3]. The phosphorylated histone H2AX (γ-H2AX) significantly overlaps with BRCA1 following DNA damage, and BRCA1-γ-H2AX foci are thought to be sites of DNA repair [26]. BRCA1 relocalization to damage-induced foci coincides with its phosphorylation [3]. Importantly, BRCA1 phosphorylation is regarded as being upstream to the signaling cascade first elicited by ATM which in turn leads to damage-induced downstream events [35]. In the present study, we found that the ratio of phosphorylated BRCA1 (p-BRCA1 Ser1423 and Ser1524) is elevated and that increased p-BRCA1 levels are a marker of the DDR and DNA repair dysfunction in both mutant Htt (Q111) cells and in a mouse model of HD. ATM may be essential for regulating the intracellular localization of BRCA1 in HD cells. Of note, the phosphorylation of both ATM and BRCA1 in response to DNA damage was reduced in HD cells compared to controls.

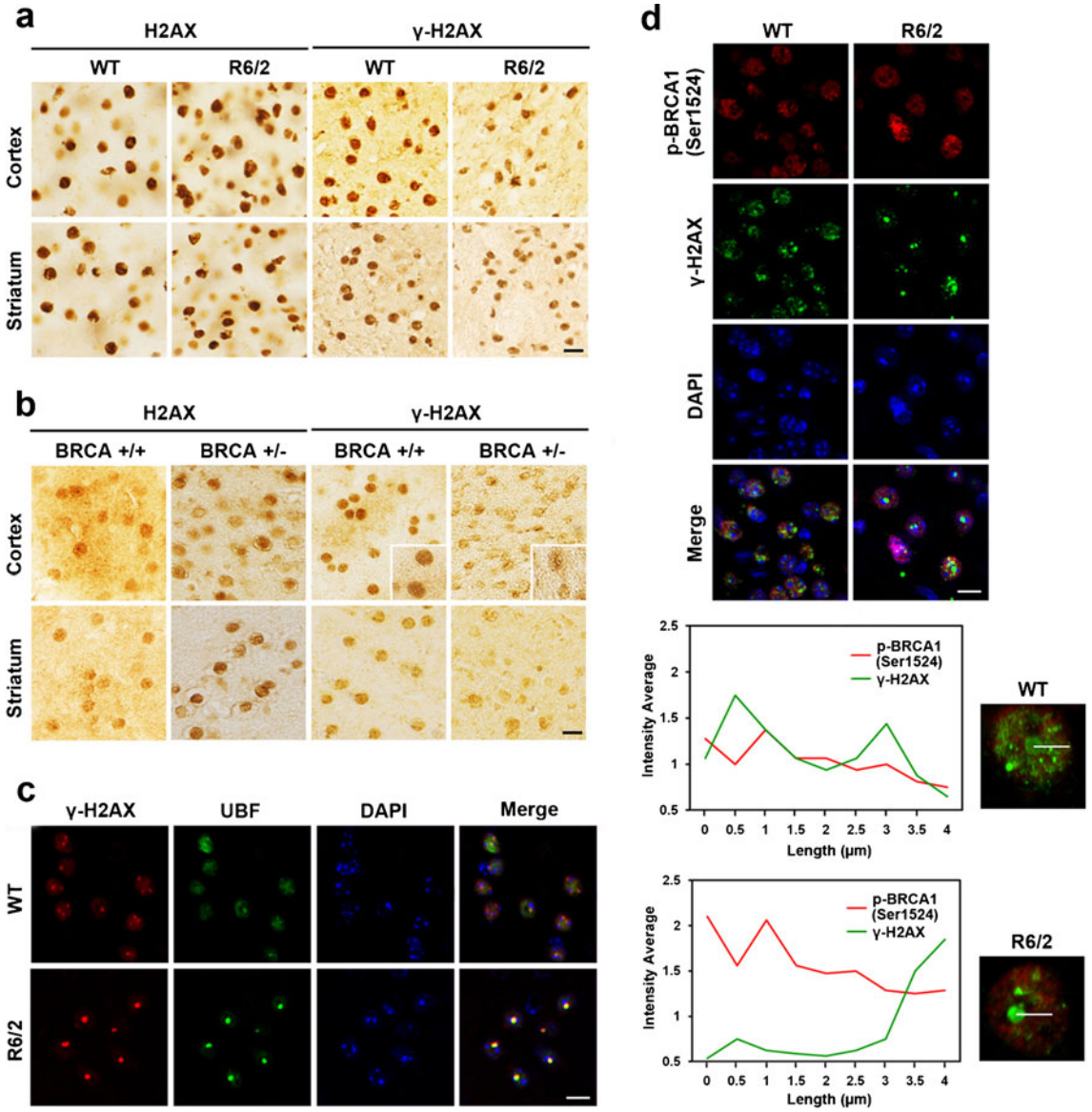

Fig. 5 The levels of pBRCA1 (Ser 1524) and γ-H2AX are altered in HD mice and BRCA$^{+/-}$ mice. **a** γ-H2AX levels were decreased in the cortex and striatum of R6/2 HD mice compared to littermate controls. **b** γ-H2AX immunoreactivity was decreased in the cortex and striatum of BRCA1 heterozygous knockout (BRCA$^{+/-}$) mice compared to WT (BRCA$^{+/+}$) mice. **c** γ-H2AX and UBF were colocalized in striatal neurons of WT and R6/2 HD mice. **d** Confocal microscopy revealed that the colocalization of pBRCA1 (Ser1524) and γ-H2AX was differentially regulated in the nucleus of WT and R6/2 HD mice. *Scale bars*: **a**–**d**, 10 μm

The BRCA1-Dependent Spatiotemporal Dynamics of γ-H2AX Is Impaired in HD

H2AX and its phosphorylated form, γ-H2AX, are fundamental chromatin components involved in DNA repair. Despite many studies investigating γ-H2AX foci in relation to DNA damage, little is known about γ-H2AX foci in normal cells in the absence of DNA damage. Our immunostaining method using detergent treatment enabled us to detect discrete and punctuate γ-H2AX immunoreactivity with typically prominent nucleolar accumulations in both control and HD cells. We found that the γ-H2AX immunoreactivity is constitutively present in the absence of DNA damage response. Consistent with this result, subcellular fractionation and Western analysis confirmed that both H2AX and γ-H2AX are localized in the nucleolus as well as in the nucleus. Interestingly, upon CPT-induced DNA damage, γ-H2AX relocalized from the nucleolus to the nucleoplasm where sites of DNA repair exist. This new finding suggests that γ-H2AX may be involved in the maintenance of ribosomal DNA under normal conditions and that it can be redistributed and translocalized to sites of DNA DSBs when DNA damage occurs in the nucleus.

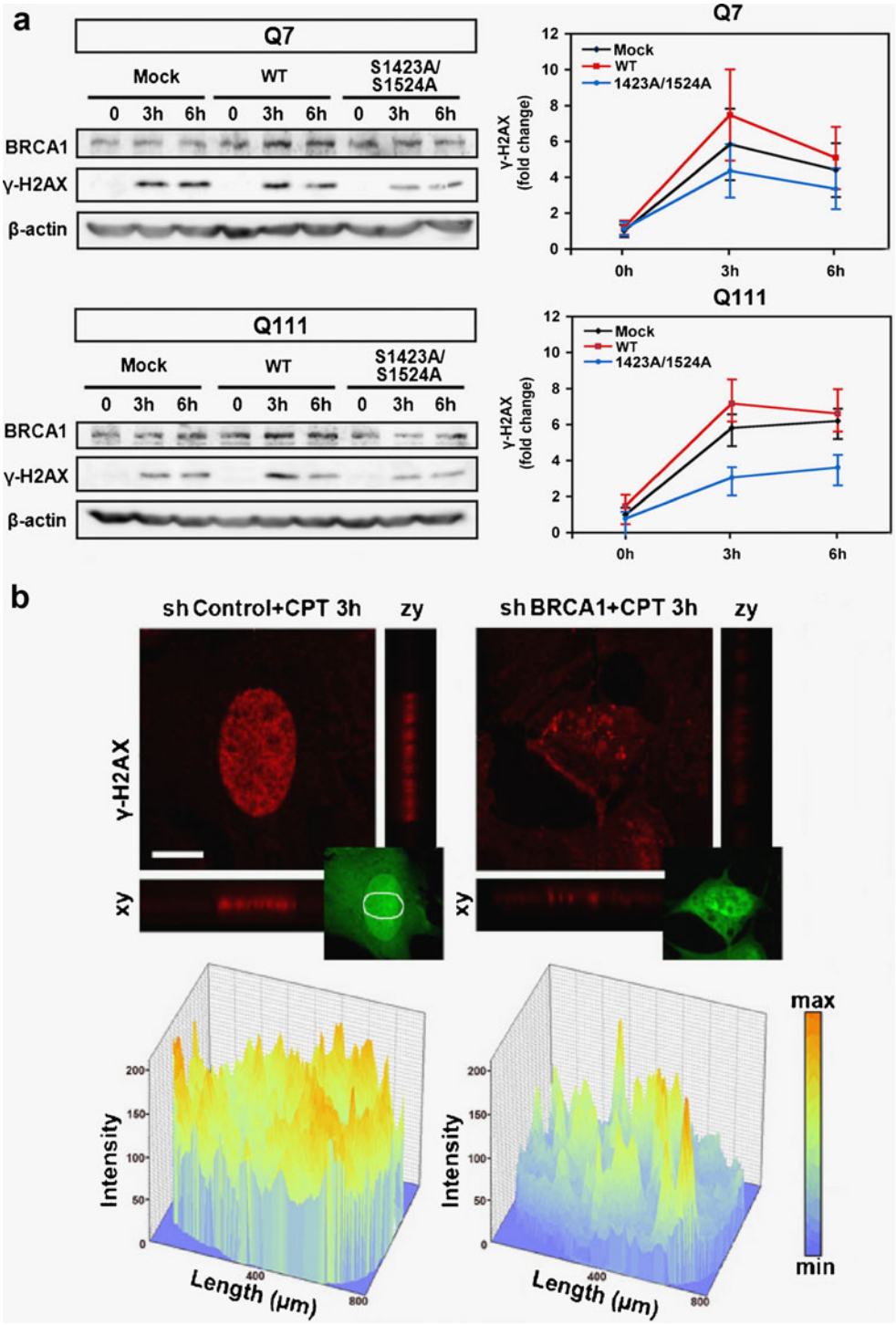

Fig. 6 BRCA1 modulates the spatiotemporal dynamics of γ-H2AX and DNA damage response. **a** The overexpression of WT-BRCA1 (WT) increased the level of γ-H2AX in Q111 HD cells in response to DNA damage but mutant BRCA1 (S1423/S1524A) did not. Cells were transfected with either WT or mutant BRCA1 (S1423/S1524A) for 48 h and then treated with CPT (10 μM) for the indicated period of time. The data represent an average of three separate experiments. **b** BRCA1 knockdown altered the spatiotemporal dynamics of γ-H2AX foci in the nucleus. Cells were transiently transfected with either shRNA control or shBRCA1 and exposed to CPT-induced DNA damage. *Upper panel*: images taken by confocal microscopy, *lower panel*: histogram analysis of the γ-H2AX images from *upper panel*. *Scale bar*: 10 μm

DNA damage-induced phosphorylation of BRCA1 modulates its physical association with other components to facilitate the DNA repair processes [35]. In this study, we provide direct evidence that the BRCA1 C-terminal (BRCT) repeat domain interacts with both H2AX and γ-H2AX. In vitro GST pull-down assay and in vivo immunoprecipitation confirm that the BRCT domain of BRCA1 recognizes γ-H2AX. In HD (Q111) cells, we found that the diffuse distribution of γ-H2AX is altered at an early stage of DNA damage response. In these cells, BRCA1 phosphorylation is delayed, and the diffuse distribution of p-BRCA1 persists. These findings are consistent with biochemical evidence of the CPT-induced foci pattern of γ-H2AX and p-BRCA1, which

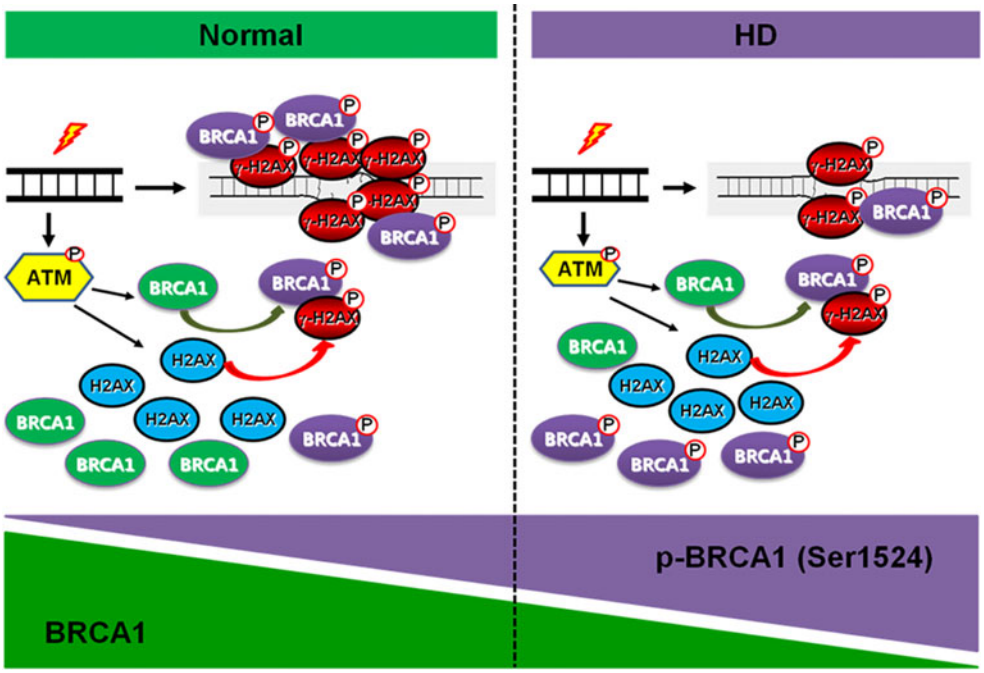

Fig. 7 A proposed scheme illustrating a BRCA1 and γ-H2AX-dependent DNA repair mechanism in neurons of normal and HD conditions. The phosphorylation status of BRCA1 is imbalanced in normal versus HD striatal cells. In turn, the BRCA1-dependent spatiotemporal dynamics of γ-H2AX foci are deregulated in HD cells in response to genotoxic stress. As a result, the BRCA1 and γ-H2AX-dependent DNA repair pathway is dysfunctional, and DNA damage is exacerbated in HD cells

persists in HD cells. In addition, knockdown of BRCA1 by shRNA impaired its function in nonhomologous end joining via γ-H2AX, which consequently increases TUNEL-positive double-strand break accumulation. Given that one of the earliest molecular responses to DNA double-strand breaks is the recruitment of γ-H2AX to sites of DNA damage, the altered spatiotemporal dynamics of γ-H2AX associated with BRCA1 deficiency suggests that it is a critical factor necessary for the assembly of the DNA repair complex that acts by distributing γ-H2AX. It seems likely that the arrival of BRCA1 and γ-H2AX to sites of DNA damage is precisely regulated to initiate the repair of damaged DNA under normal conditions. In contrast, cells with a deficiency of BRCA1 or an imbalance of BRCA1/p-BRCA1, as occurs in HD, manifest delayed redistribution of γ-H2AX that in turn exacerbates the accumulation of DNA damage-induced double-strand breaks (Fig. 7). This delayed activation of the DDR may contribute to neuronal dysfunction and neurodegeneration in HD [32]. Which double-strand break repair pathway, a nonhomologous end joining or a homology-directed repair, is dominated by BRCA1 in neurodegenerative conditions remains to be determined.

In conclusion, our data show that levels of p-BRCA1 and γ-H2AX are indicators of DDR activation in HD. BRCA1 deficiency contributes to neuronal injury in HD by interfering with the spatiotemporal redistribution of γ-H2AX that normally occurs in response to DNA damage. Our findings suggest that modulation of BRCA1 may, therefore, improve DDR in HD and ameliorate disease progression.

Materials and Methods

Plasmid Constructs

The S140A and S140E mutations in Mcherry-C1-H2AX Vector were created by using the KOD-Plus-Mutagenesis Kit (TOYOBO, Japan). The mutations were verified by sequencing.

GST Pull-down Assay

GST pull-down assay using cell lysates of H2AX-transfected Q7 and Q111 cells was performed as previously described [36].

Cell Culture and DNA Damage

ST$Hdh^{Q7/7}$ (wild type) and ST$Hdh^{Q111/111}$ (HD knock-in striatal cell line expresses mutant huntingtin at endogenous level) were generously provided from Dr. Marcy MacDonald (Harvard Medical School) [37]. Cells were treated with camptothecin (CPT; 10 μM; Sigma, St. Louis, MO) for the indicated period of time.

RNA Interference Experiment

Four shRNA-BRCA1 expression plasmids were purchased from OriGene Technologies (Rockville, MD). These vectors were constructed in pRS under U6 promoter control using the following target sequence in each of the vector: (1) 5′-

AAATGCCAGTCAGGCACAGCAGAAACCTA-3′, (2) 5′-TGGCACTCAGGAAAGTATCTCGTTACTGG-3′, (3) 5′-AAGGAACCTGTCTCCACAAAGTGTGACCA-3′, and (4) 5′-AGGACCTGCGAAATCCAGAACAAAGCACA-3′. Cells were seeded and allowed to attach for 24 h before transfection with either shRNA-BRCA1 or control shRNA by using the transfection reagent supplied by the manufacturer and according to the instructions provided by the manufacturer (Lipofectamine^{TM} LTX and PLUS Reagents, Invitrogen Life Technologies, Frederick, MD) for 48 h.

Animals

The male R6/2 mice were bred with females from their background strain (B6CBAFI/J), and offspring were genotyped using PCR [30, 38, 39]. CAG repeat length remained stable within a 147–153 range. Female mice were used in the experimental paradigms. Brain tissues of BRCA1 heterozygous knockout (BRCA$^{+/-}$) and wild-type (BRCA$^{+/+}$) mice were generously provided by Dr. Wen-Hwa Lee (University of California, Irvine School of Medicine) [18].

Subcellular Fraction

Cell pellet was washed with PBS and centrifuged at 1,000 rpm for 4 min at 4°C. Pellet was resuspended in 500 μl of ice-cold buffer (10 mM HEPES-KOH, pH 7.9, 1.5 mM $MgCl_2$, 10 mM KCL, 0.5 mM DTT, and protease inhibitors), kept on ice for 5 min, and Dounce homogenized 20 times using a tight pestle. Dounced pellets were centrifuged at 1,000 rpm for 5 min at 4°C to pellet nuclei and other fragments. The supernatant can be retained as the cytoplasmic fraction. The nuclear pellet was resuspended in 300 μl 0.25 M sucrose and 10 mM $MgCl_2$ and layered over 300 μl 0.35 M sucrose and 0.5 mM $MgCl_2$ and centrifuged at 2,500 rpm for 5 min at 4°C. This step results in a cleaner nuclear pellet. The clean, pelleted nuclei were resuspended in 300 μl 0.35 M sucrose and 0.5 mM $MgCl_2$ and sonicated six times, 10 s each time using Bioruptor. The sonicated sample was then layered over 300 μl 0.88 M sucrose and 0.5 mM $MgCl_2$ and centrifuged at 3,500 rpm for 10 min at 4°C. The pellet contains the nucleoli, and the supernatant can be retained as the nucleoplasmic fraction. The nucleoli was resuspended in 350 mM RIPA buffer and centrifuged at 14,000 rpm for 10 min at 4°C.

Flow Cytometry Analysis

Harvested cells were treated with a reagent in accordance with the instruction provided by the manufacturer (FITC Annexin V Apoptosis Detection Kit), and stained cells were analyzed using a FACSort flow cytometer (BD Biosciences, San Jose, CA). Graphs were exported as TIF images and assembled in Photoshop.

Histopathological Evaluation

Brain tissue sections were immunostained for BRCA1, phospho-BRCA1 (Ser1423), phospho-BRCA1 (Ser1524), H2AX, and γ-H2AX using a previously reported conjugated secondary antibody method. Preabsorption with excess target proteins, omission of the primary antibodies, and omission of secondary antibodies were performed to determine the amount of background generated from the detection assay.

Confocal Microscopy

Immunofluorescence staining and confocal microscopy were used to determine the ATM (Santa Cruz Biotech), p-ATM (Ser1981) (Upstate Biotech), BRCA1 (Santa Cruz Biotech), phospho-BRCA1 (Ser1423) (Santa Cruz Biotech), phospho-BRCA 1 (Santa Cruz Biotech; Ser1524), H2AX (Santa Cruz Biotech), and γ-H2AX (Upstate Biotech). The specimens were incubated for 1 h with DyLight 594 donkey anti-rabbit IgG antibody, DyLight 488 donkey anti-goat IgG antibody, and DyLight 488 donkey anti-mouse IgG antibody (Jackson ImmunoResearch, Baltimore Pike, PA, USA; 1:400) after the incubation of primary antibody. Images were analyzed using an Olympus FluoView FV10i confocal microscope (Olympus, Tokyo, Japan). Control experiments were performed in the absence of primary antibody or in the presence of blocking peptide.

Western Blot Analysis

Western blot was performed as previously described [40]. A total of 30 μg of protein was subjected to SDS–PAGE and blotted with anti-ATM, anti-p-ATM (Ser1981), anti-BRCA1, anti-phospho-BRCA1 (Ser1423), anti-phospho-BRCA1 (Ser1524), anti-H2AX, and anti-γ-H2AX antibodies. Protein loading was controlled by probing for β-actin (Santa Cruz Biotech) on the same membrane. The densitometry of protein intensity was performed by an imaging analyzer (LAS-3000; Fuji, Tokyo, Japan).

Immunoprecipitation Analysis

Cell pellets were suspended in a lysis buffer containing protease inhibitors, and lysates were centrifuged at 14,000 rpm for 10 min. Equal amounts of protein were precipitated with ATM, BRCA1, phospho-BRCA1 (Ser1524), and H2AX. The procedures were performed as previously described [40].

Terminal Deoxynucleotidyl Transferase dUTP Nick End Labeling Assay

To detect CPT-induced neuronal DNA damage, we cultured Q7 and Q111 striatal cells on 24-well plates. Cells were treated with 10 μM CPT for 12 and 24 h, fixed by 4 % PFA, and the apoptotic cells by DNA double-strand breaks were detected using TUNEL staining kit (ApopTag Fluorescein In Situ Apoptosis Detection Kit, CHEMICON International, Inc.). The apoptotic cells in four fields per slide were examined under an Olympus epifluorescence microscope (Olympus, Tokyo, Japan) at ×20 objective magnification.

Statistical Analysis

Data were analyzed by Prism software (GraphPad Software, San Diego, CA, USA) using either Student's *t* test or one-way analysis of variance followed by a Newman–Keuls post hoc test. Data are presented as the mean±SEM. Differences were considered statistically significant when $p<0.05$.

Acknowledgments We thank Dr. Marcy MacDonald (Harvard Medical School) for ST*Hdh*$^{Q7/7}$ and ST*Hdh*$^{Q111/111}$ cells. This study was supported by WCU Neurocytomics Program Grant (800–20080848) (H.R.) and SRC Grant (2010-0029-403) (H.R.) from KOSEF, NIH NS 067283-01A1 (H.R.), and R01CA79892 (TO), R01CA90631 (TO), and Susan G. Komen Breast Cancer Research Award (TO).

References

1. Coppedè F, Migliore L (2010) DNA repair in premature aging disorders and neurodegeneration. Curr Aging Sci 3:3–19
2. Kovtun IV, Liu Y, Bjoras M, Klungland A, Wilson SH, McMurray CT (2007) OGG1 initiates age-dependent CAG trinucleotide expansion in somatic cells. Nature 447:447–452
3. Scully R, Chen J, Ochs RL, Keegan K, Hoekstra M, Feunteun J, Livingston DM (1997) Dynamic changes of BRCA1 subnuclear location and phosphorylation state are initiated by DNA damage. Cell 90:425–435
4. Deng CX, Wang RH (2003) Roles of BRCA1 in DNA damage repair: a link between development and cancer. Hum Mol Genet 12 (suppl 1):R113–R123
5. Ljungman M, Lane DP (2004) Transcription—guarding the genome by sensing DNA damage. Nat Rev Cancer 4:727–737
6. Starita LM, Parvin JD (2003) The multiple nuclear functions of BRCA1: transcription, ubiquitination and DNA repair. Curr Opin Cell Biol 15:345–350
7. Venkitaraman AR (2001) Functions of BRCA1 and BRCA2 in the biological response to DNA damage. J Cell Sci 114:3591–3598
8. Chen Y, Farmer AA, Chen CF, Jones DC, Chen PL, Lee WH (1996) BRCA1 is a 220-kDa nuclear phosphoprotein that is expressed and phosphorylated in a cell cycle-dependent manner. Cancer Res 56:4074
9. Ruffner H, Verma IM (1997) BRCA1 is a cell cycle-regulated nuclear phosphoprotein. Proc Natl Acad Sci USA 94:7138–7143
10. Cortez D, Wang Y, Qin J, Elledge SJ (1999) Requirement of ATM-dependent phosphorylation of brca1 in the DNA damage response to double-strand breaks. Science 286:1162–1166
11. Lee JS, Collins KM, Brown AL, Lee CH, Chung JH (2000) hCds1-mediated phosphorylation of BRCA1 regulates the DNA damage response. Nature 404:201–204
12. Scully R, Ganesan S, Vlasakova K, Chen J, Socolovsky M, Livingston DM (1999) Genetic analysis of BRCA1 function in a defined tumor cell line. Mol Cell 4:1093–1099
13. Bachelier R, Xu X, Wang X, Li W, Naramura M, Gu H, Deng CX (2003) Normal lymphocyte development and thymic lymphoma formation in Brca1 exon-11-deficient mice. Oncogene 22:528–537
14. Cao L, Li W, Kim S, Brodie SG, Deng CX (2003) Senescence, aging, and malignant transformation mediated by p53 in mice lacking the Brca1 full-length isoform. Genes Dev 17:201–213
15. Gowen LC, Johnson BL, Latour AM, Sulik KK, Koller BH (1996) Brca1 deficiency results in early embryonic lethality characterized by neuroepithelial abnormalities. Nat Genet 12:191–194
16. Hakem R, de la Pompa JL, Sirard C, Mo R, Woo M, Hakem A, Wakeham A, Potter J, Reitmair A, Bilia F et al (1996) The tumor suppressor gene Brca1 is required for embryonic cellular proliferation in the mouse. Cell 85:1009–1023
17. Hohenstein P, Kielman MF, Breukel C, Bennett LM, Wiseman R, Krimpenfort P, Cornelisse C, van Ommen GJ, Devilee P, Fodde R (2001) A targeted mouse Brca1 mutation removing the last BRCT repeat results in apoptosis and embryonic lethality at the headfold stage. Oncogene 20:2544–2550
18. Liu CY, Flesken-Nikitin A, Li S, Zeng Y, Lee WH (1996) Inactivation of the mouse Brca1 gene leads to failure in the morphogenesis of the egg cylinder in early postimplantation development. Genes Dev 10:1835–1843
19. Ludwig T, Chapman DL, Papaioannou VE, Efstratiadis A (1997) Targeted mutations of breast cancer susceptibility gene homologs in mice: lethal phenotypes of Brca1, Brca2, Brca1/Brca2, Brca1/p53, and Brca2/p53 nullizygous embryos. Genes Dev 11:1226–1241
20. Ludwig T, Fisher P, Ganesan S, Efstratiadis A (2001) Tumorigenesis in mice carrying a truncating Brca1 mutation. Genes Dev 15:1188–1893
21. Shen SX, Weaver Z, Xu X, Li C, Weinstein M, Chen L, Guan XY, Ried T, Deng CX (1998) A targeted disruption of the murine Brca1 gene causes gamma-irradiation hypersensitivity and genetic instability. Oncogene 17:3115–3124
22. Xu X, Weaver Z, Linke SP, Li C, Gotay J, Wang XW, Harris CC, Ried T, Deng CX (1999) Centrosome amplification and a defective G2-M cell cycle checkpoint induce genetic instability in BRCA1 exon 11 isoform-deficient cells. Mol Cell 3:389–395
23. Xu X, Wagner KU, Larson D, Weaver Z, Li C, Ried T, Hennighausen L, Wynshaw-Boris A, Deng CX (1999) Conditional mutation of Brca1 in mammary epithelial cells results in blunted ductal morphogenesis and tumour formation. Nat Genet 22:37–43
24. Xu X, Qiao W, Linke SP, Cao L, Li WM, Furth PA, Harris CC, Deng CX (2001) Genetic interactions between tumor suppressors Brca1 and p53 in apoptosis, cell cycle and tumorigenesis. Nat Genet 28:266–271
25. Redon C, Pilch D, Rogakou E, Sedelnikova O, Newrock K, Bonner W (2002) Histone H2A variants H2AX and H2AZ. Curr Opin Genet Dev 12:162–169
26. Paull TT, Rogakou EP, Yamazaki V, Kirchgessner CU, Gellert M, Bonner WM (2000) A critical role for histone H2AX in recruitment of repair factors to nuclear foci after DNA damage. Curr Biol 10:886–895
27. Celeste A, PetersenS RPJ, Fernandez-Capetillo O, Chen HT, Sedelnikova OA, Reina-San-Martin B, Coppola V, Meffre E, Difilippantonio MJ et al (2002) Genomic instability in mice lacking histone H2AX. Science 296:922–927
28. Stucki M, Clapperton JA, Mohammad D, Yaffe MB, Smerdon SJ, Jackson SP (2008) MDC1 directly binds phosphorylated histone

H2AX to regulate cellular responses to DNA double-strand breaks. Cell 133:549
29. Tauchi H, Kobayashi J, Morishima K, van Gent DC, Shiraishi T, Verkaik NS, van Heems D, Ito E, Nakamura A, Sonoda E et al (2002) Nbs1 is essential for DNA repair by homologous recombination in higher vertebrate cells. Nature 420:93–98
30. Mangiarini L, Sathasivam K, Seller M, Cozens B, Harper A, Hetherington C, Lawton M, Trottier Y, Lehrach H, Davies SW et al (1996) Exon1 of the HD gene with an expanded CAG repeat is sufficient to cause a progressive neurological phenotype in transgenic mice. Cell 87:493–506
31. Giuliano P, De Cristofaro T, Affaitati A, Pizzulo GM, Feliciello A, Crscuolo C, De Michele G, Filla A, Awedimento EV, Varrone S (2003) DNA damage induced by polyglutamine-expanded proteins. Hum Mol Genet 12:2301–2309
32. Illuzzi J, Yerkes S, Parekh-Olmedo H, Kmiec EB (2009) DNA breakage and induction of DNA damage response proteins precede the appearance of visible mutant huntingtin aggregates. J Neurosci Res 87:733–747
33. Gatei M, Scott SP, Filippovitch I, Soronika N, Lavin MF, Weber B, Khanna KK (2000) Role for ATM in DNA damage-induced phosphorylation of BRCA1. Cancer Res 60:3299–3304
34. Gatei M, Zhou BB, Hobson K, Scott S, Young D, Khanna KK (2001) Ataxia telangiectasia mutated (ATM) kinase and ATM and Rad3 related kinase mediate phosphorylation of Brca1 at distinct and overlapping sites. In vivo assessment using phospho-specific antibodies. J Biol Chem 276:17276–17280
35. Foray N, Marot D, Gabriel A, Randrianarison V, Carr AM, Perricaudet M, Ashworth A, Jeggo P (2003) A subset of ATM- and ATR-dependent phosphorylation events requires the BRCA1 protein. EMBO J 22:2860–2871
36. Ouchi M, Fujiuchi N, Sasai K, Katayama H, Minamishima YA, Ongusaha PP, Deng C, Sen S, Lee SW, Ouchi T (2004) BRCA1 phosphorylation by Aurora-A in the regulation of G2 to M transition. J Biol Chem 279:19643–19648
37. Trettel F, Rigamonti D, Hilditch-Maguire P, Wheeler VC, Sharp AH, Persichetti F, Cattaneo E, MacDonald ME (2000) Dominant phenotypes produced by the HD mutation in STHdh (Q111) striatal cells. Hum Mol Genet 9:2799–2809
38. Ryu H, Lee J, Zaman K, Kubilis J, Ferrante RJ, Ross BD, Neve R, Ratan RR (2003) Sp1 and Sp3 are oxidative stress-inducible, anti-death transcription factors in cortical neurons. J Neurosci 23:3597–3606
39. Ryu H, Lee J, Hagerty SW, Soh BY, MacAlpin SE, Cormier KA, Smith KM, Ferrante RJ (2006) ESET/SETDB1 gene expression and histone H3 (K9) trimethylation in Huntington's disease. Proc Natl Acad Sci USA 103:19176–19181
40. Ryu H, Jeon GS, Cashman NR, Kowall NW, Lee J (2011) Differential expression of c-Ret in motor neurons versus non-neuronal cells is linked to the pathogenesis of ALS. Lab Invest 91:342–352